Journal of Marine Science and Application (2019) 18:530–541
https://doi.org/10.1007/s11804-019-00109-2

RESEARCH ARTICLE

Design of Heading Fault-Tolerant System for Underwater Vehicles Based on Double-Criterion Fault Detection Method

Yanhui Wei[1] · Jing Liu[1] · Shenggong Hao[1] · Jiaxing Hu[1]

Received: 4 August 2018 / Accepted: 19 December 2018 / Published online: 24 October 2019

Abstract
This paper proposes a heading fault tolerance scheme for operation-level underwater robots subject to external interference. The scheme is based on a double-criterion fault detection method using a redundant structure of a dual electronic compass. First, two subexpansion Kalman filters are set up to fuse data with an inertial attitude measurement system. Then, fault detection can effectively identify the fault sensor and fault source. Finally, a fault-tolerant algorithm is used to isolate and alarm the faulty sensor. The program can effectively detect the constant magnetic field interference, change the magnetic field interference and small transient magnetic field interference, and conduct fault tolerance control in time to ensure the heading accuracy of the system. Test verification shows that the system is practical and effective.

Keywords Underwater robot · Heading fault tolerance · Redundant structure · Double-criteria failure detection · Federated Kalman filter · Electronic compass

1 Introduction

Remotely operated vehicles (ROVs) are among the important equipment for deep-sea exploration and exploitation. Accurate and reliable attitude detection systems are essential for an entire job-level ROV system (Babcock and Zinchuk 1990). However, as the scale of the system expands, the failure rate also increases. The fault tolerance of the system is an important guarantee of the accuracy and reliability of the attitude detection system (Cui et al. 2011). Thus, fault-tolerant analysis of the system is necessary to determine its fault source and reduce the impact of the fault on the attitude detection system in a timely and accurate manner. Heading information is an important element of the attitude detection system; thus, studying the heading fault tolerance of the ROV attitude detection system is important.

As a result of errors in the inertial device, errors in the inertial navigation system accumulate over time in the calculation update, and errors in the system output information continue to increase. An electronic compass can calculate the heading, which is typically a combination of a magnetometer and a tilt sensor. The electronic compass is highly susceptible to magnetic field interference (Fang et al. 2011, Ritz et al. 2009) in an underwater unknown environment, and its working-level encounters difficulty in fulfilling the navigation needs of ROVs. Therefore, the inertial attitude detection system and electronic compass combined navigation method can be used to obtain reliable heading information. Furthermore, peripheral devices can be added to correct the heading accuracy of the system.

In recent years, combined attitude detection systems have used the information in the Kalman filter (KF) (Li et al. 2011) to detect faults directly. Some commonly used methods are the following: state test method (Blanke et al. 2006), residual test method (Gao et al. 2011), fault detection method based on adaptive KF (Hajiyev 2012), and fault detection method based on particle filter (Caron et al. 2007, Arulampalam and Maskell 2002). Feng Sun et al. (Sun et al. 2005) adopted the structure of the centralized KF and state test method for system fault tolerance of integrated navigation.

Article Highlights • Propose a double criterion fault detection method to detect electronic compass failure;
• Perform fault pre-judgment before determining the fault to increase the real-time performance of fault detection;
• Under the condition of constant magnetic field interference, changing magnetic field interference and small transient magnetic field interference, fault detection, and fault-tolerant control are carried out to ensure the reliability of heading information.

✉ Yanhui Wei
15663423085@163.com

[1] College of Automation, Harbin Engineering University, Harbin 150001, China

Yueqian Liang et al. (Liang and Jia 2015) used a generalized Kalman filter (EKF) and deformed differential KF to control aircraft system faults and measurement faults in a fault-tolerant manner. Bo Zhao et al. (Zhao et al. 2014) used the hidden Markov model (Crisan and Rozovskii 2011) to model the system and the particle filter method to detect the faults of the ROV driver and sensor. Le et al. (Le and Matunaga 2014) identified the fault sources in the combined attitude detection system using different states of the fault detection quantities in the unscented KF (Cheng et al. 2010) and quaternion estimator.

Many scholars have conducted significant work in ROV fault detection and system fault tolerance (Norgaard et al. 2000, Bar-Shalom et al. 2001, Mohajerin and Lygeros 2015), but most of the research objects are long-standing faults (Esfahani and Lygeros 2016) that are difficult to recover by themselves. This study investigates the situation in which the electronic compass is susceptible to the influence of the surrounding magnetic field and generates erroneous data. This approach is expected to quickly and accurately determine whether the electronic compass is in a normal working state or a fault state as well as perform timely fault-tolerant control to ensure the heading accuracy of the system.

In this paper, the fault-tolerant scheme of the ROV heading system is designed from the aspects of sensor fault detection, adaptive regulation, sensor redundancy configuration, and data distributed fusion. The proposed double-criterion fault detection method is used to detect the electronic compass fault. This method has the following advantages: (1) it pre-judges the fault before judging the fault, thereby increasing the real-time performance of the fault detection. (2) Compared with the residual χ^2 test method, the electronic compass double-criterion fault detection method not only effectively detects the fault information of the heading but also analyzes the relationship between the two fault criteria to determine the cause of system interference. (This interference is one of the following types: changing magnetic field interference, constant magnetic field interference, or small transient magnetic interference.) (3) The dual electronic compass redundancy structure using the federated Kalman filter (FKF) can flexibly distribute the information of the attitude detection system and has high fault tolerance.

2 Overall Structural Design of ROV Heading System

2.1 Design of ROV Heading System

Heading information is critical for ROV deep-sea operations. The electronic compass is susceptible to environmental interference to improve the reliability of the navigation system. The ROV system heading information is measured using a MEMS attitude measurement system and dual electronic compass redundancy configuration.

The system hardware configuration uses the electronic compass HMR3000 and ADIS16405 three-axis magnetometer to provide geomagnetic heading as a double compass. As system reliability is a concern in this system, the FKF is adopted as the data fusion scheme, and the best feedback-free mode (Gao et al. 2014) with no fault tolerance is selected. Its structure is shown in Fig. 1.

FK filtering is a piecewise estimation, two-step cascaded information fusion technique. The system is structurally composed of two subfilters (FF1 and FF2) and a main filter. Based on the assumption that the strapdown inertial navigation system (SINS) has the highest reliability and is used as a reference (Julier and Durrant-Whyte 2002), the other subsystems form a plurality of subfilters that are executed in parallel with the reference system and output local measurement information optimal estimates based on the observations provided by the subsystem. The output information of each local filter is finally optimized in the main filter to obtain a global estimate of the heading system.

In Fig. 1, FF1 consists of SINS and HMR3000 and FF2 consists of SINS and ADIS16405. The state quantities of FF1 and FF2 are the same, as shown in the following equation:

$$X_{\mathrm{yaw},k} = [\Delta\psi \;\; \Delta\varepsilon_Z]^{\mathrm{T}} \tag{1}$$

where $\Delta\psi$ is the heading angle increment, and $\Delta\varepsilon_Z$ is the zero offset increment of the gyro at time k and k-1. The equation of state, observation equation, filter gain matrix, error variance matrix, and one-step prediction estimation variance matrix are shown in the following equation:

$$\begin{gathered} X_{\mathrm{yaw},k} = j_{\mathrm{yaw}|k,k-1}X_{\mathrm{yaw},k-1} + G_{\mathrm{yaw}|k,k-1}W_{\mathrm{yaw}|k,k-1} \\ Z_{\mathrm{yaw},k} = H_{\mathrm{yaw},k}X_{\mathrm{yaw},k} + V_{\mathrm{yaw},k} \\ K_{\mathrm{yaw},k} = P_{\mathrm{yaw}|k,k-1}H_{\mathrm{yaw}}^{\mathrm{T}}\left(H_{\mathrm{yaw}}P_{\mathrm{yaw}|k,k-1}H_{\mathrm{yaw}}^{\mathrm{T}} + R_{\mathrm{yaw}}\right)^{-1} \\ P_{yaw|k,k-1} = j_{\mathrm{yaw}}P_{\mathrm{yaw}|k,k-1}j_{\mathrm{yaw}}^{\mathrm{T}} + G_{\mathrm{yaw}}Q_{\mathrm{yaw}}G_{\mathrm{yaw}}^{\mathrm{T}} \\ P_{\mathrm{yaw},k} = \left(I - K_{\mathrm{yaw}}H_{\mathrm{yaw}}\right)P_{\mathrm{yaw}|k,k-1} \end{gathered} \tag{2}$$

The state transition matrix and noise drive matrix are

$$\varphi_{\mathrm{yaw}} = \begin{bmatrix} 1 & -\Delta t \\ 0 & 1 \end{bmatrix}, \quad \Gamma_{\mathrm{yaw}} = \begin{bmatrix} -1 & 0 \\ 0 & 1 \end{bmatrix}.$$

The noise excitation sequence and state noise variance matrix are

$$W_{\mathrm{yaw}} = [\, n_{\omega r} \quad n_{\omega w} \,]^T, \quad Q_{\mathrm{yaw}} = \begin{bmatrix} \sigma_{Zr}^2\Delta t & \sigma_{Z_w}^2\Delta t^2 \\ \sigma_{Z_w}^2\Delta t^2 & \sigma_{Z_w}^2\Delta t \end{bmatrix}.$$

The observation of the transfer matrix is

$$H_{\mathrm{yaw}} = [\, 1 \quad 0 \,].$$

V_k is the observation process noise, and the observation of FF1 consists of the difference between the heading angle $\psi_{\mathrm{Mag}}$of the MAG1 and the heading angle $\psi$of the system at

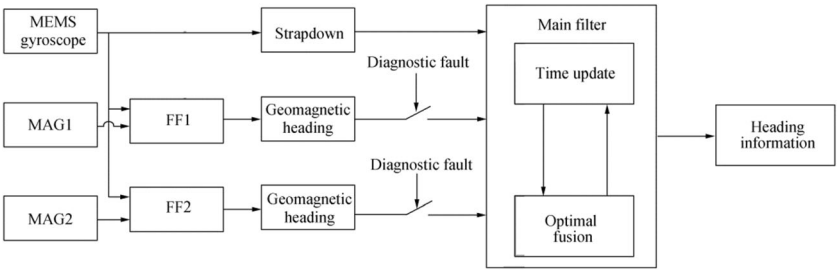

Fig. 1 Structure of ROV heading system

the previous moment. Therefore, the measurement noise variance matrix is

$$Z_{\text{yaw},k} = \left(\psi_{Mag1} - \psi\right), \quad R_{\text{yaw}} = \sigma^2_{Mag1}.$$

The observation and measurement noise variance matrix of subfilter FF2 is

$$Z_{\text{yaw},k} = \left(\psi_{Mag2} - \psi\right), \quad R_{\text{yaw}} = \sigma^2_{Mag2}.$$

2.2 Design of System Compensation Scheme

Owing to the complexity of the underwater environment, the electronic compass is susceptible to interference from ferromagnetic materials when the ROV is operating underwater. If the attitude and heading reference (AHR) part of the navigation system adopts the traditional observation model, errors would occur in the roll and pitch angle outputs when the magnetometer is disturbed. Furthermore, when the electronic compass is subjected to strong interference, the attitude output of the system diverges, thereby resulting in failure of the attitude and heading information.

Therefore, to avoid the impact on the attitude information of the system when the electronic compass fails, the observation model is corrected and compensated in the system. The steps in the compensation plan are as follows:

In the conventional AHR system model, the observation uses the difference between the measured values of the accelerometer and magnetometer as well as the local gravity field and magnetic field intensity projected in the carrier coordinate system as observations. The observation Z_{ahrs} and observation transfer matrices H_{ahrs} are shown in the following equation:

$$Z_{ahrs} = \begin{bmatrix} a_x - a_x \\ a_y - a_y \\ a_z - a_z \\ m_x - m_x \\ m_y - m_y \\ m_z - m_z \end{bmatrix} \quad H_{ahrs} = \begin{bmatrix} \dfrac{\partial a}{\partial X_{ahrs}} \\ \dfrac{\partial m}{\partial X_{ahrs}} \end{bmatrix} \tag{3}$$

where a and m are the measured values of the accelerometer and magnetometer, respectively; and a and m are the projections of the local gravity field and local magnetic field in the carrier coordinate system, respectively.

1a Using the original data of the three-axis magnetometer and the three-axis accelerometer, we calculate the heading angle in the geographic coordinate system. Then, we use this angle as the observation information of the navigation system heading.

Tilt compensation for the three-axis raw data of the electronic compass is presented in the following equation:

$$\begin{aligned} \begin{bmatrix} h_x \\ h_y \\ h_z \end{bmatrix} &= \left[R_{pitch}\right]^{\mathrm{T}} \left[R_{roll}\right]^{\mathrm{T}} \begin{bmatrix} m_x \\ m_y \\ m_z \end{bmatrix} \\ &= \begin{bmatrix} 1 & 0 & 0 \\ 0 & \cos q & \sin q \\ 0 & -\sin q & \cos q \end{bmatrix}^{\mathrm{T}} \begin{bmatrix} \cos g & 0 & -\sin g \\ 0 & 1 & 0 \\ \sin g & 0 & \cos g \end{bmatrix}^{\mathrm{T}} \begin{bmatrix} m_x \\ m_y \\ m_z \end{bmatrix} \end{aligned} \tag{4}$$

where $\begin{bmatrix} h_x & h_y & h_z \end{bmatrix}^{\mathrm{T}}$ is the magnetic field information of the horizontal plane, and $\begin{bmatrix} m_x & m_y & m_z \end{bmatrix}^{T}$ is the magnetic field strength measured in the geographic coordinate system.

The heading angle is calculated as follows:

$$y_{\text{Mag}} = arctan\frac{h_y}{h_x} \tag{5}$$

2a The observation model of the attitude heading part of the integrated navigation system is corrected.

For the system attitude measurement, the difference between the measured value of the accelerometer and the projection of the local gravity field in the carrier coordinate system is determined. Then, the heading observation uses the difference between the heading angle ψ_{Mag} calculated by the system based on the observation information and heading angle ψ obtained by the state update.

According to the preceding steps, including a 4D observation measurement, the observation equation can be expressed as

$$Z_k = H_k X_k \tag{6}$$

where

$$Z_{ahrs} = \begin{bmatrix} a_x - a_x \\ a_y - a_y \\ a_z - a_z \\ y_{\mathrm{Mag}} - y \end{bmatrix}, \quad H_{ahrs} = \begin{bmatrix} \dfrac{\partial a}{\partial X_{ahrs}} & 0 \\ 0 & 1 \end{bmatrix}.$$

3a According to the preceding filtering result, the roll amp; pitch angles are obtained by the quaternion. The quaternion, which is obtained through filtering with the corrected heading angle, completes the filter observation update.

To verify the feasibility of the compensation scheme, the navigation system was placed at rest, and the electronic compass was subjected to ferromagnetic interference from 1.1 to 4.6 s. The attitude and heading information of the navigation system before and after compensation was recorded to verify the effectiveness of the scheme. The Euler angle waveform before and after system compensation is shown in Fig. 2.

As shown in Fig. 2, when the electronic compass is subjected to ferromagnetic interference, the roll and pitch angles of the system before the model is uncompensated producing a steady-state error of − 13° and 28°, respectively. The roll and pitch angles of the system after the compensation measures are still maintained at the initial angle. This experiment verified not only the problems in the original scheme but also the feasibility of the compensation scheme.

3 Fault-Tolerant Design of ROV Heading System

The fault-tolerant system can detect real-time information of the filters in the heading system and determine if the system is operating properly. It is also the premise of fault diagnosis and isolation and system reconstruction, which directly affects the accuracy of the entire attitude detection system (Poulsen and Ravn 2000).

The ROV heading fault-tolerant system scheme designed in this paper is shown in Fig. 3. As the figure shows, the fault-tolerant system includes redundant sensor structure fault tolerance, subsystem fault detection and isolation, and fault-tolerant synthesis algorithm.

The fault detection algorithm in the local filter first confirms the fault of the subsystem, and then determines the faulty position and attitude detection system. Once the failure of a subsystem has been determined, the state estimate obtained by the corresponding local filter is incorrect and cannot be input to the main filter. In this case, the main filter calculates the estimated value of the system error state using the state estimate of the other local filter, and simultaneously takes measures such as fault repair or switching channels to repair the failed attitude detection system. Until the failed attitude detection system is repaired, the local filter can obtain the correct local state estimate and input it to the main filter. The combined

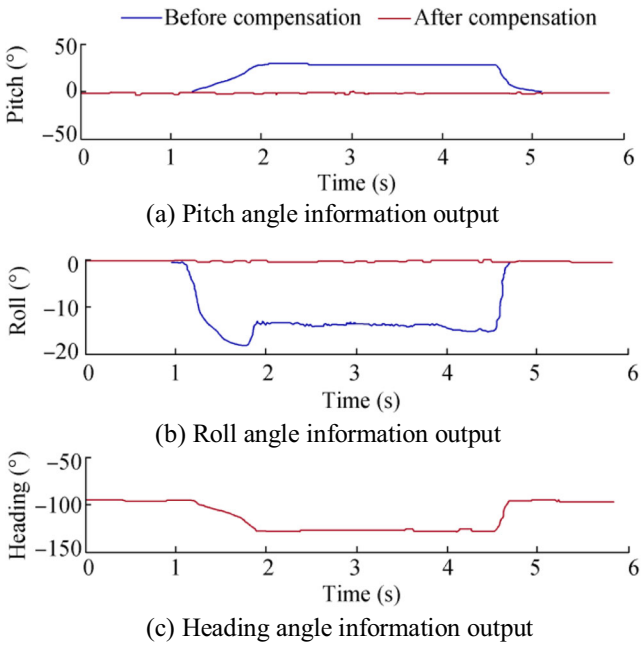

Fig. 2 Attitude waveform diagram of integrated navigation system before and after compensation. **a** Pitch angle information output; **b** roll angle information output; **c** heading angle information output

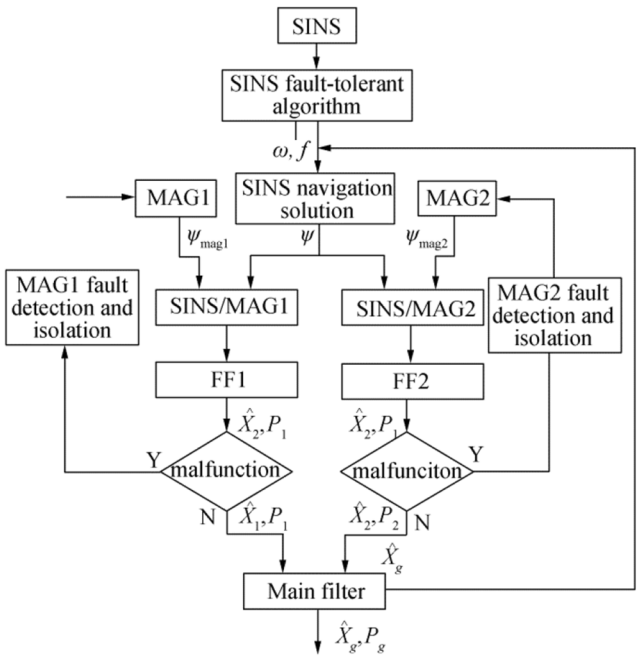

Fig. 3 Schematic of ROV heading fault-tolerant system

attitude detection system at this time re-provides the user with reliable and accurate heading information.

3.1 Double Fault Detection Method

To effectively detect the fault information of the heading, the heading angle variation model of the electronic compass measurement and heading angle change measured by the inertial device are established. The heading fault detection system in the ROV attitude detection system judges the fault condition of the system based on the difference between the two.

The heading angle change of the electronic compass that is working without failure is modeled in the following equation:

$$\Delta\theta_m(t) = \theta_m(t) - \theta_m(t-1) + \mu_m(t) - \mu_m(t-1) \tag{7}$$

where $\Delta\theta_m(t)$ is the change of the heading angle from t-1 to t, $\theta_m(t)$ is the heading angle of the electronic compass at time t, and $\mu_m(t)$ is the noise in the heading angle of the system at time t.

The heading angle increment is obtained by integrating the angular velocity of the Z-axis MEMS gyro at time t, which is modeled in the following equation:

$$\Delta\theta_g(t) = (\omega_U(t) + \mu_U(t)) \cdot \Delta t \tag{8}$$

where $\omega_U(t)$ is the angular velocity of the Z-axis of the system at time t, $\mu_U(t)$ is the noise in the Z-axis angular velocity information of the MEMS gyro, and Δt is the sampling period of the system.

$e(t)$ indicates the error between the two, and the following equation shows the relationship between the two:

$$e(t) = \Delta\theta_m(t) - \Delta\theta_g(t) \tag{9}$$

Equation (5) is averaged to reduce the effects of white noise (Zheng et al. 2006), as shown in the following equation:

$$e(t) = \frac{1}{n} \sum_{m=-n+1}^{0} e(t_n + m \cdot \Delta t) \tag{10}$$

When the electronic compass in the system is free from external interference, the value $e(t)$ of Eq. (6) obeys a normal distribution with a mean of 0. When the electronic compass is disturbed by external factors, $\Delta\theta_m(t)$ changes rapidly, and $e(t)$ no longer obeys the normal distribution; thus, the fault information of the heading angle can be obtained. The fault detection of the electronic compass can be achieved by setting a reasonable threshold for $e(t)$.

When the fault detection parameter is calculated, because it is the average of the difference between the angular increment of the electronic compass and the angular increment obtained by integrating the MEMS Strapdown Inertial Navigation System over a period of time, the system encounters a certain delay in fault identification. Adding the fault pre-judgment link in the fault detection scheme can ensure the real-time performance of the heading angle fault detection scheme.

When the external magnetic field interferes with the system, the heading angle of the electronic compass changes rapidly, but it does not affect the heading angle obtained by integrating the MEMS inertial device. Using the difference between the two can achieve fault prediction as shown in the following equation:

$$\Delta\varphi_s(t) = \varphi_m(t) - \varphi_g(t) \tag{11}$$

When the system is operating normally, the random noise of the MEMS gyro causes accumulation errors. However, the error accumulation of the heading angle obtained by integrating the gyro in a short time is small and negligible compared with the heading sudden change generated when the electronic compass is disturbed by external factors. Therefore, the fault pre-judgment (Zhen and Feng 2005) can be performed by detecting $\Delta\varphi_s(t)$.

When the fault pre-judgment is conducted, the fault pre-judgment time is set to $t_{\text{error}} = a \cdot \Delta t$. Once $\Delta\varphi_s(t)$ exceeds the threshold, the heading filter immediately stops the observation update process. At this time, to prevent the fault information of the heading angle from affecting the attitude detection system, the system only obtains the heading angle information through the state update. After the fault pre-judgment time t_{error}, if the system detects a fault in the electronic compass, the fault processing is performed. If the electronic compass fault is not detected, it switches to the normal mode.

As $e(t)$ and $\Delta\varphi_s(t)$ obey the normal distribution with a mean of 0 when no fault exists, they can be normalized first, and then the corresponding threshold is calculated by the set false alarm probability to identify the fault. For details, refer to "Research on Threshold Selection Principle Based on Sensor Fault Detection" (Wang 2009). When a fault has been identified, we can analyze the relationship between the two fault criteria to obtain the cause of the fault, and take corresponding measures to reduce the impact of the fault.

After fault prediction or detection, if a steady-state error exists between the heading angle output by the attitude detection system and the heading angle of the electronic compass,

Table 1 Electronic compass double-criterion fault detection judgment logic

Electronic compass failure	Fault pre-judgment	Fault judgment
No failure	No	No
No failure	Yes → No	No
Varying magnetic field interference	Yes	Yes
Constant magnetic field interference	Yes	Yes → No

the information of the heading attitude detection system should be re-initialized to eliminate the heading angle steady-state error caused by the fault phase.

According to the two failure criteria, the judgment logic of the double-criterion failure detection is shown in Table 1.

Table 1 shows that the electronic compass double-criterion fault detection method has two functions: (1) effectively detecting the fault information of the heading and (2) analyzing the cause of the system interference by examining the relationship between the two failure criteria.

3.2 Fault-Tolerant Synthesis Algorithm

In the fault-tolerant scheme of the system, the residual sensor structure is used to improve the reliability of the SINS, and the double-criteria fault detection method is adopted, the purpose of which is to ensure the reliability of the heading information in the combined attitude detection system. Therefore, by detecting the fault of the subsystem, we can determine which type of attitude detection system has failed.

The fault judgment criteria are shown in Table 2.

When one of the electronic compasses fails, the double-criteria fault detection method can detect the fault and alarm in time. At this time, the heading information output from the subfilter that detected the fault is not input to the main filter. The main filter uses the heading information output by another subsystem filter for reliable heading state estimation. After the fault is removed, the heading information output by the faulty subsystem is restored to normal. The information is re-entered into the main filter, which then returns to its previous normal operating state.

If the two electronic compasses fail at the same time, then the system only calculates the heading according to the SINS system. When the failure of the subsystem is repaired, the output data of the normally operating subsystem is input to the main filter, and the entire system resumes normal operation.

The error state estimates and variances obtained by the two subfilters are X_1, P_1 and X_2, P_2, respectively. When the system is running normally, the global state estimation and variance are as shown in the following equations:

$$X_g = P_g\left(P_1^{-1}X_1 + P_2^{-1}X_2\right) \tag{12}$$

$$P_g = \left(P_1^{-1} + P_2^{-1}\right)^{-1} \tag{13}$$

If the subsystem SINS/MAG1 (filter FF1) fails, then a fault message appears in X_1. The fault subsystem is isolated and the state of the primary system is estimated as follows:

$$X_g = X_2 \tag{14}$$

The output of the failed subsystem is shown in the following equation:

$$Z_1 = H_1 X_g \tag{15}$$

If the subsystem SINS/MAG2 (filter FF2) fails, then the state of the system is estimated as

$$X_g = X_1 \tag{16}$$

The failure subsystem output is estimated to be

$$Z_2 = H_2 X_g \tag{17}$$

If both SINS/MAG1 and SINS/MAG2 fail, then the state estimation of the system can only use the heading information obtained through the gyro integration. At this time, the state of the system is estimated as follows:

$$X_{g,t} = X_{g,t-1} + \omega_D \bullet \Delta t \tag{18}$$

Where $X_{g,t}$ is the heading information of the current time, $X_{g,t-1}$ is the heading information of the previous moment, ω_D is the angular rate of the grounding to the gyro in the NED coordinate system, and Δt is the updating period of the attitude detecting system.

4 Simulation

First, the double-criteria fault detection method used in the case of electronic compass failure is simulated in various situations. Then, the residual χ^2 test method and double-criterion fault detection method are compared to illustrate the feasibility and effectiveness of the electronic compass double-criterion fault detection scheme. Finally, the entire ROV heading fault-tolerant system is simulated to verify the

Table 2 Criteria for system failure judgment

Fault status	Judgment of failure	Update output
The system is trouble free	MAG1 and MAG1 have not failed	FF1 and FF2
SINS/MAG1 has failed	MAG1 fails but MAG2 is faultless	FF2
SINS/MAG2 has failed	MAG1 is faultless but MAG2 is faulty	FF1
SINS/MAG1 and SINS/MAG2 have failed	MAG1 fails and MAG2 fails	SINS

effectiveness of the heading fault-tolerant system designed in this study.

4.1 Simulation of Electronic Compass Double-Criterion Fault Detection Method

The failure of the electronic compass includes the following: changing magnetic field interference, constant magnetic field interference, and small transient magnetic interference. The following is a simulation of the three cases using the electronic compass double-criterion fault detection method (see Fig. 4):

1a The heading angle error of the working-level ROV electronic compass constantly changes due to the interference of the changing magnetic field. The fault status of the system can be detected by fault pre-judgment and fault judgment. When a fault is detected, the heading information of the electronic compass is invalid. In this case, on the one hand, the system reports the fault condition to the host and warns the ROV to leave the magnetic field interference area as soon as possible; on the other hand, the observation update processing of the heading KF is no longer performed, and the heading angle is updated using only the method of *Z*-axis gyroscope integration.

To verify the effectiveness of the scheme, the ROV attitude detection system is placed at rest. In simulating the changing magnetic field interference by constantly moving a ferromagnetic substance near an electronic compass, the simulation data waveforms of the electronic compass heading angle and fault detection state in the experiment are shown in Figs. 5 and 6.

Figures 5 and 6 present experimental images of electronic compass failure detection under ferromagnetic interference conditions. Numerous experiments show that when the electronic compass is interfered by the ferromagnetic material, an angular error of more than 5° occurs. When the ferromagnetic material continues to interfere, the electronic compass has an angular increment error greater than 60°/s.

Therefore, the threshold of the electronic compass failure prediction is set to 5°, the threshold of the failure judgment is set to 60°/s, and the prediction duration t_{error} is set to 0.1 s in the experiment. The ferromagnetic substance was used to interfere with the electronic compass at 0.7–0.9 s and 2.09–2.3 s. After the disturbance occurs, the heading angle error and angular increment error increase rapidly. Once the threshold is exceeded, the fault pre-judgment and fault judgment respond quickly. The system can quickly isolate the electronic compass information containing the fault information and update the heading information only through the gyro integral. After troubleshooting, the heading angle of the electronic compass can be repeatedly used to observe and update the system, and the attitude detection system resumes normal operation.

2a The electronic compass heading angle error of the working compass ROV is constant when subjected to constant magnetic field interference. Therefore, the fault prediction of the system is always in a fault state. When a fault is detected, the system enters a fault state and returns to normal after a certain period. In this case, on the one hand, the fault is reported to the host and the ROV is prompted to leave the magnetic interference zone as soon as possible; on the other hand, in the attitude detection system, the observation update processing of the heading KF is stopped and only the *Z*-axis gyroscope integration is used. Thereafter, the heading angle is updated.

To verify the effectiveness of the program, the ROV combined attitude detection system is placed at rest, and the constant magnetic field interference is simulated by placing a ferromagnetic substance near the electronic compass. The interference source is removed after a certain period. The data waveforms of the electronic compass heading angle and fault detection state in the experiment are shown in Figs. 7 and 8.

Figures 7 and 8 present images of the failure detection test of the electronic compass in the case of ferromagnetic interference. In the experiment, the threshold of the electronic compass failure pre-judgment was set to 5°, the threshold of the failure judgment was set to 60°/s, and the failure pre-judgment duration t_{error} was set to 0.1 s. The magnetic substance interferes with the electronic compass in 2–7.2 s.

As shown in Fig. 7, the heading angle error and angle increment error increase rapidly after the occurrence of interference. Once the threshold is exceeded, the fault pre-judgment and fault judgment respond immediately. The attitude detection system quickly isolates the electronic compass information containing the fault information and uses the gyro integral to update the heading information.

As shown in Fig. 8, at 2.38 s, the heading angle error tends to be stable, the fault pre-judgment flag is maintained in the fault state, the angular increment error is rapidly reduced below the threshold value, the fault judgment flag is set to 0, and the system enters the constant magnetic field interference state. When the ferromagnetic material is removed in 7.2 s, the heading angle quickly returns to normal, the angular increment changes sharply, the fault pre-judgment flag and fault judgment flag position is 0, and the system releases the fault state. The attitude detection system re-observes the heading angle of the electronic compass and the system returns to the normal state.

3a When the electronic compass is subjected to small transient magnetic interference, the electronic compass is subjected to short interference time, the influence of the system magnetic field is small, and the fault pre-judgment and fault judgment threshold of the electronic compass are not exceeded. To reliably utilize the heading reference information provided by the

Fig. 4 HMR3000 electronic compass

electronic compass in this state, with reference to the accelerometer adaptive scheme processing method, we can construct the reliability parameter σ_m by the residual of the heading angle.

The residual value of the heading angle is λ_m, and the adaptive equation is constructed as

$$\sigma_m = k_m \lambda_m \tag{19}$$

where k_m is the set weighting factor and constructs the covariance σ_m^2. The larger the value of covariance σ_m^2, the stronger the influence of the external magnetic field on the carrier and the lower the credibility of the system to the electronic compass. Otherwise, the trust level is higher. By changing the covariance matrix $\boldsymbol{R}$ in this manner, the system can achieve a relatively stable heading output when transient magnetic interference occurs outside the system.

To ensure that the EKF filter does not cause the system output to diverge due to σ_m^2 in the adaptive adjustment, σ_m^2 should be limited, and the simulation verification is limited to $0.15 \leq \sigma_m^2 \leq 1$.

The attitude detection system is installed on the carrier, and the adaptive scheme effect of the heading portion of the attitude detection system is verified. The comparison of the effects before and after adopting this scheme is shown in Fig. 9.

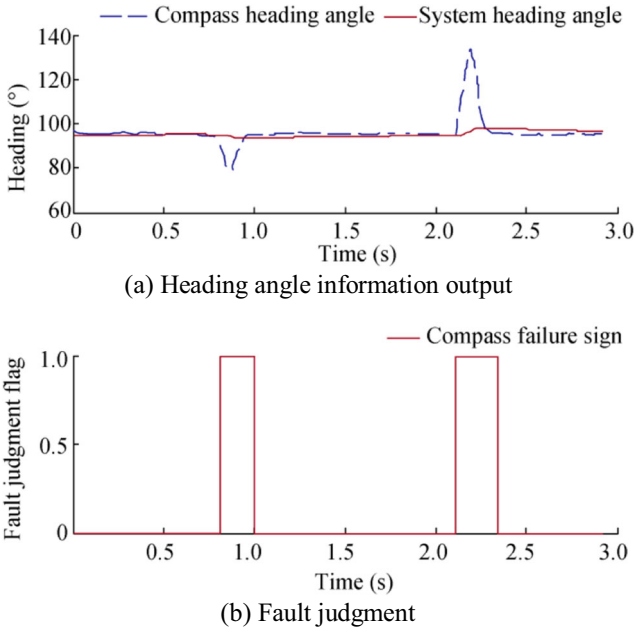

(a) Heading angle information output

(b) Fault judgment

Fig. 5 Heading angle information output and fault judgment. **a** Heading angle information output; **b** fault judgment

As shown in Fig. 9, when the electronic compass adaptive parameter is within the set range, the system performs adaptive adjustment. Before and after the adaptive scheme, the heading angle error is significantly reduced compared with the condition before the adaptive scheme is implemented. The heading angle waveform is smoother and the noise is reduced compared with the condition before the adaptive scheme is performed. Thus, the adaptive adjustment scheme achieves an improved filtering effect.

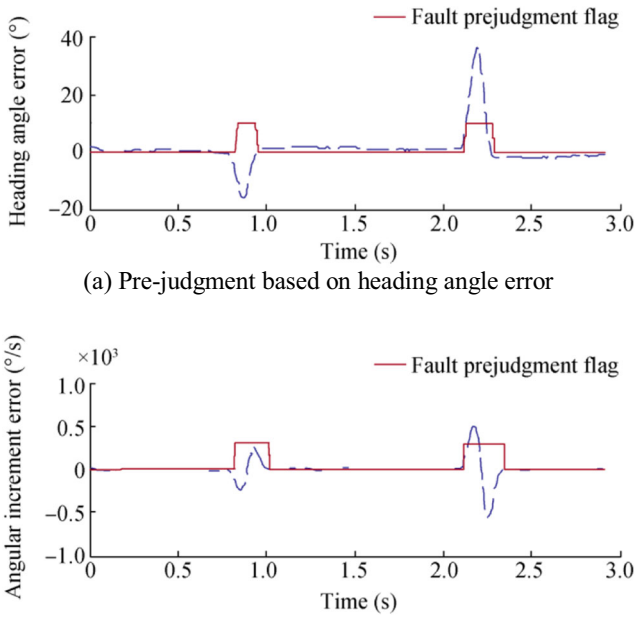

(a) Pre-judgment based on heading angle error

(b) Pre-judgment based on angular increment error

Fig. 6 Double-criteria fault detection. **a** Pre-judgment based on heading angle error; **b** pre-judgment based on angular increment error

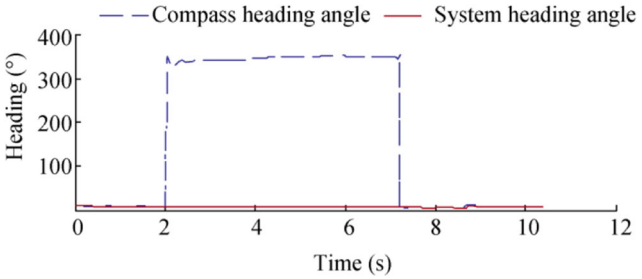

(a) Heading angle information output

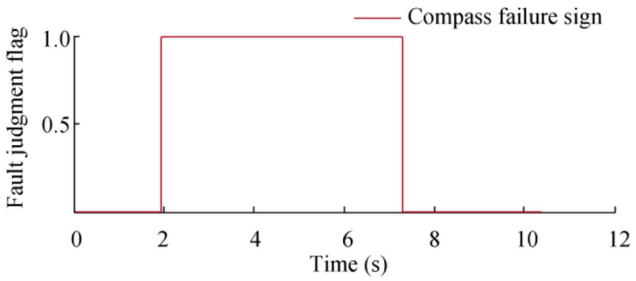

(b) Fault judgment

Fig. 7 Heading angle information output and fault judgment. **a** Heading angle information output; **b** fault judgment

4.2 Comparison of Results of Electronic Compass Double-Criterion Fault Detection Method and Residual χ^2 Test Method

In this experiment, the residual χ^2 test method and the proposed double-criteria fault detection method are compared to verify the feasibility and effectiveness of the electronic compass double-criterion fault detection scheme.

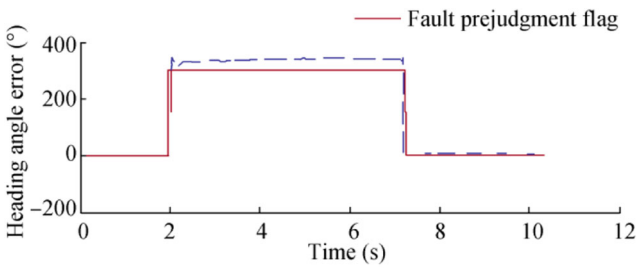

(a) Pre-judgment based on heading angle error

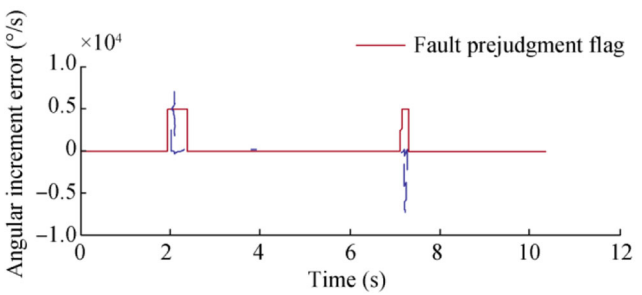

(b) Pre-judgment based on angular increment error

Fig. 8 Double-criteria fault detection**. a** Pre-judgment based on heading angle error; **b** pre-judgment based on angular increment error

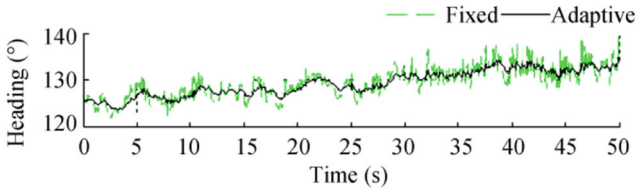

(a) Comparison of heading angle adaptive effects

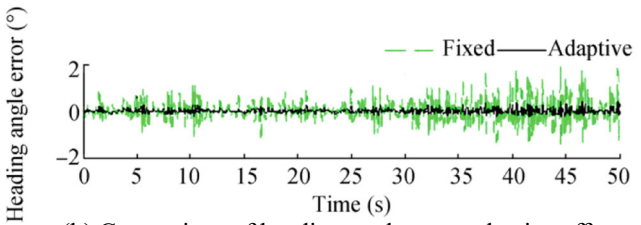

(b) Comparison of heading angle error adaptive effects

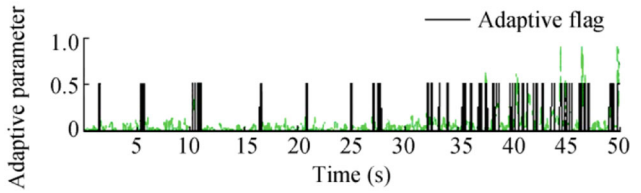

(c) Adaptive parameter

Fig. 9 Comparison of electronic compass covariance adaptive effect. **a** Comparison of heading angle adaptive effects; **b** comparison of heading angle error adaptive effects; **c** adaptive parameter

In the parameter setting, the failure threshold in the residual χ^2 test is set to $T_D = 1$, and the threshold of the electronic compass failure prediction in the double-criterion detection method is 5°. The fault judgment threshold is 60°/s, and the fault pre-judgment duration t_{error} is 0.1 s. The attitude

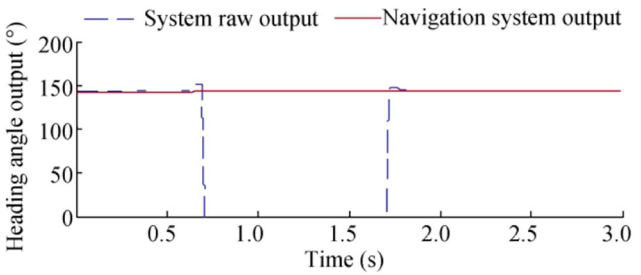

(a) Comparison of heading angle output

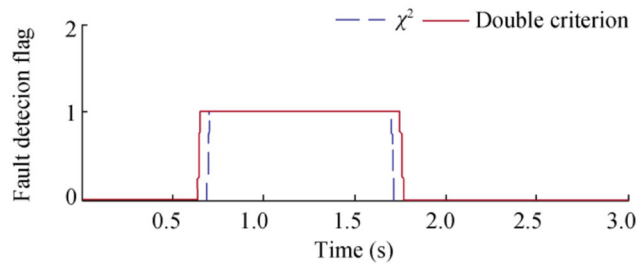

(b) Comparison of fault detection flags

Fig. 10 Comparison of residual test method and electronic compass double-criterion fault detection method. **a** Comparison of heading angle output; **b** comparison of fault detection flags

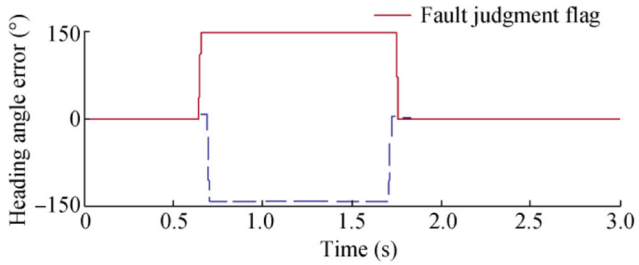

(a) Fault pre-judgment

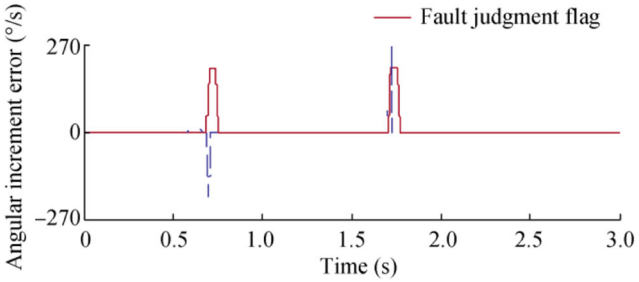

(b) Fault judgment

Fig. 11 Electronic compass double-criterion fault detection fault pre-judgment and fault judgment. **a** Fault pre-judgment; **b** fault judgment

detection system is placed at rest, and the HMR3000 electronic compass is continuously disturbed by ferromagnetic materials in 0.64 to 1.83 s. At the same time, the original heading information of the ROV attitude detection system, output heading information of the system, output data of the residual χ^2 detection method, and fault flag of the electronic compass are recorded. The waveforms drawn by the experimental data are presented in Figs. 10 and 11.

As shown in Fig. 10, at 0.64 s and 1.79 s, the HMR3000 electronic compass is disturbed by magnetic substances. When the interference source leaves the electronic compass, the heading information of the attitude detection system returns to normal. Starting from 0.68 s and continuing until 1.71 s, the residual detection method detects the fault information of the HMR3000 electronic compass. However, failure information at 0.64–0.68 s and 1.72–1.76 s was not detected using this method; the angular error of the electronic compass was 5° or more. The double-criteria fault detection method detects not only the fault information of the HMR3000 electronic compass in 0.65–1.75 s but also that in 0.64–0.68 s and 1.72–1.76 s.

As shown in Fig. 11, the fault pre-judgment flag of the system continues for a long time, and the fault flag of the system changes rapidly after the system is disturbed, and then gradually decreases to normal after the interference received by the electronic compass becomes constant. Table 1 shows that the HMR3000 is subject to constant magnetic field interference.

Compared with the residual test method, the electronic compass double-criterion fault detection method not only effectively detects the fault information of the heading but also finds the cause of system interference by analyzing the relationship between the two fault criteria. Therefore, the electronic compass double-criterion fault detection method is adopted as the fault detection scheme for the heading angle of the ROV attitude detection system.

4.3 Simulation of ROV Heading Fault-Tolerant System

The dual-compass redundant ROV combined attitude detection system is placed at rest and the ferromagnetic material is placed nearby to simulate magnetic field interference. The source of interference is removed after a short period. MAG1 is the heading information output by the three-axis magnetometer ADIS16405, and MAG2 is the heading information output by the electronic compass HMR3000. The threshold for predicting the electronic compass failure is set to 5°, the threshold for fault determination is set to 60°/s, and the judgment delay is 0.1 s. In the experiment, the electronic compass heading angle, fault detection state, and heading data waveform output by the FKF are shown in Fig. 11.

As shown in Fig. 12, when no fault occurs in the attitude detection system, the state estimation of the FKF

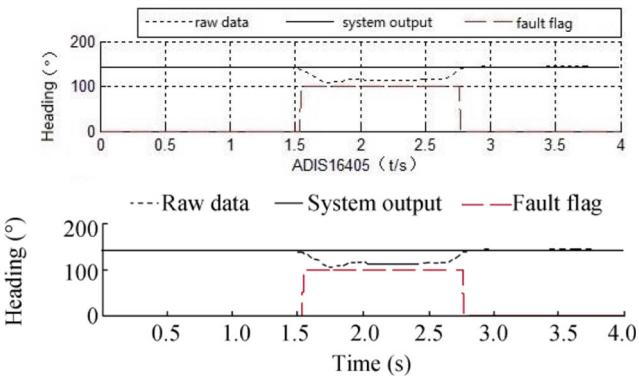

(a) ADIS16405 output heading information

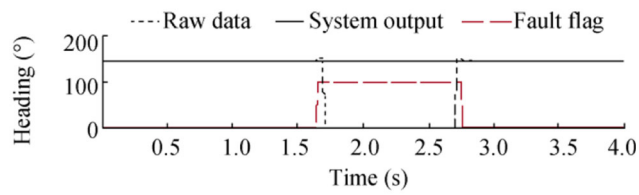

(b) HMR3000 output heading information

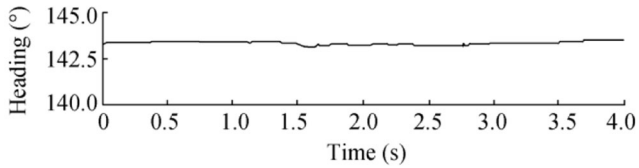

(c) Heading information output by federated Kalman filter

Fig. 12 Heading angle of FKF. **a** ADIS16405 output heading information; **b** HMR3000 output heading information; **c** heading information output by federated Kalman filter

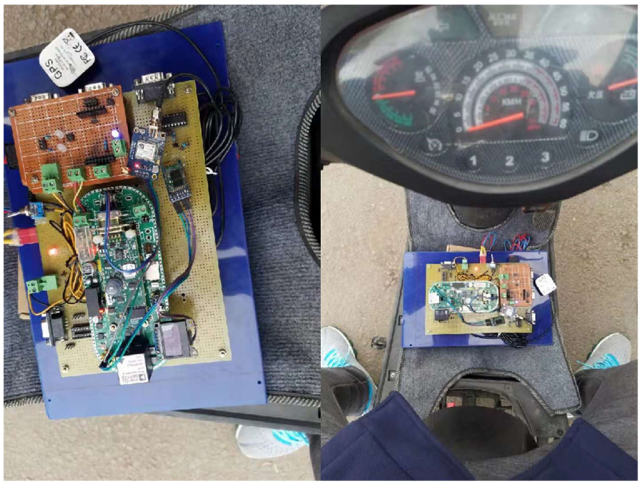

Fig. 13 Experiment on integrated navigation system

simultaneously uses the outputs of the two subfilters to calculate the heading information. At 1.46 s, the heading angle of the three-axis magnetometer ADIS16405 begins to produce errors due to interference. The local filter FF1 detects a fault in the ADIS16405 at 1.53 s, and the fault flag acts. At this time, the heading information output by the local filter FF2 is used as a state estimation of the FKF. At 1.65 s, the local filter FF2 detects the failure of the HMR3000 electronic compass, and the fault flag acts. At this time, both compasses have faults, and the heading information of the FKF of the pose detection system is obtained by gyro integration. At 2.75 s, the fault of the HMR3000 electronic compass is released, and the state of the FKF is estimated as the heading information output by the local filter FF2. At 2.76 s, the fault of the ADIS16405 is

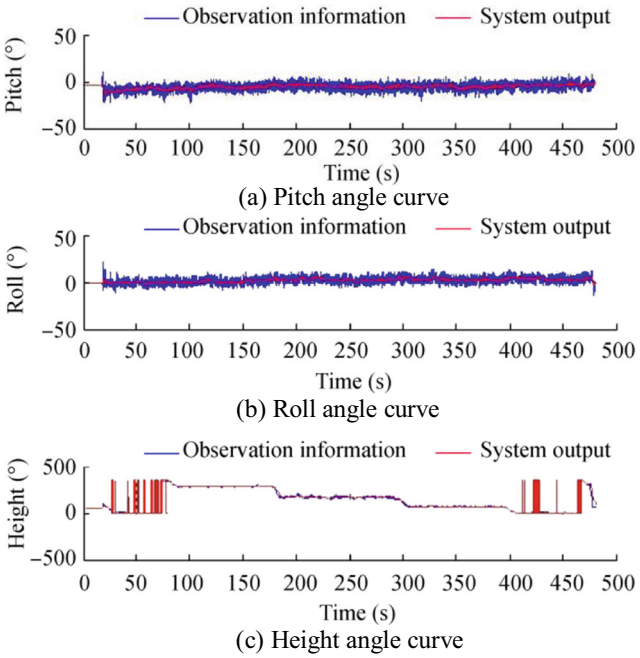

Fig. 14 Experiment on attitude waveform of navigation system. **a** Pitch angle curve; **b** roll angle curve; **c** height angle curve

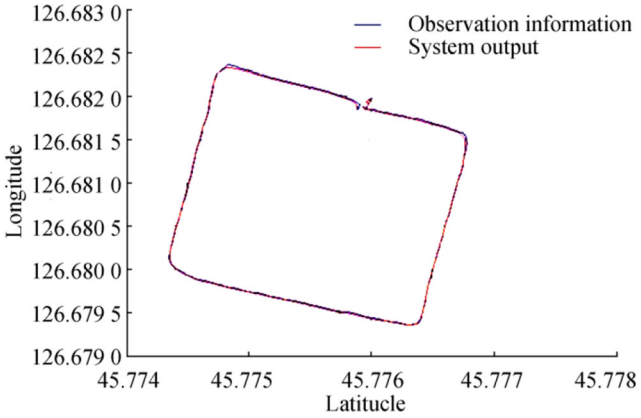

Fig. 15 Longitude and latitude curve of navigation system experiment

released, the heading information of the ROV attitude detection system returns to normal, and the state estimation of the FKF uses the output of the two subfilters to calculate the heading information. This simulation verifies the effectiveness of the FKF and bistable fault detection method in the design of the heading redundancy system of the ROV attitude detection system.

5 Verification Experiment on Integrated Navigation System

The ROV for underwater operation mainly includes modes such as fixed height, depth, direction, and uniform inspection. The ROV navigation system is required to provide attitude, heading, and speed information that meets the ROV control accuracy requirements. In this experiment, the integrated navigation system was installed on the motion carrier, and the navigation system was tested around the #61 teaching building (see Fig. 13). Considering the limitations of the test environment, this experiment uses a GPS navigation system as a reference for the speed and horizontal position of the integrated navigation system. A barometer sensor is used to provide a high reference as shown in Figs. 14 and 15.

As shown in Fig. 14, the attitude of the system remains convergent, which indicates that the system effectively filters out the data fluctuation of the accelerometer caused by the carrier vibration and obtains a highly accurate estimation of the attitude and heading. The experimental results show that the heading accuracy of the system can fulfill the information needs of underwater robots during deep-sea operations.

6 Conclusions

In this study, a dual electronic compass redundancy fault detection scheme based on double-criteria fault detection method is designed based on the FKF for the heading system of the

job-level ROV. This solution not only effectively detects and isolates faults but also accurately identifies the source of the fault. According to the detected fault information, the system can quickly make judgments, isolate the fault compass, prevent pollution of other sensors, effectively improve the reliability of the heading information, meet the needs, and guarantee the safety of deep-sea ROV operations. The simulation results show that the system verifies and isolates various types of faults and verifies the effectiveness of the designed fault-tolerant scheme. Finally, experiments validate that the system can meet the demands of navigation information for the working-level ROV in the underwater working environment.

Foundation Item This study is supported by the Natural Science Foundation of Heilongjiang Province (E2017024); 13th Five-Year Pre-Research (J040717005); National Defense Basic Research (A0420132202); and China International Ministry of Science and Technology International Cooperation Project (2014DFR10010).

References

Arulampalam MS, Maskell S, Gordon N (2002) A tutorial on particle filters for online nonlinearn-Gaussian Bayesian tracking. IEEE Trans Signal Process 50:174–188. https://doi.org/10.1109/78.978374

Babcock PSI, Zinchuk JJ (1990) Fault-tolerant design optimization: application to an autonomous underwater vehicle navigation system. Proceedings of the Autonomous Underwater Vehicle Technology, pp 34–43. https://doi.org/10.1109/AUV.1990.110435

Bar-Shalom Y, Kirubarajan T, Li XR (2011) Estimation with Applications to Tracking and Navigation.Theory, Algorithms and Software,John Wiley & Sons, Inc. https://doi.org/10.1161/HYPERTENSIONAHA.109.130880

Blanke M, Kinnaert M, Lunze DIJ (2006) Diagnosis and fault-tolerant control. Diagnosis and Fault-tolerant Control, pp 493–494. https://doi.org/10.1007/978-3-540-35653-0

Caron F, Davy M, Duflos E (2007) Particle filtering for multisensor data fusion with switching observation models: application to land vehicle positioning. IEEE Trans Signal Process 55:2703–2719. https://doi.org/10.1109/tsp.2007.893914

Cheng XQ, Qu JY, Yan ZP, Bian XQ (2010) H_∞ robust fault-tolerant controller design for an autonomous underwater vehicle's navigation control system. J Mar Sci Appl 9(1):87–92. https://doi.org/10.1007/s11804-010-8052-x

Crisan D, Rozovskiĭ BL (2011) The oxford handbook of nonlinear filtering. Oxford University Press 39(8):1849–1850. https://doi.org/10.1080/02664763.2012.680690

Cui N, Han P, Mu R (2011) Fault-tolerant integrated navigation for reusable boost vehicle based on strong tracking UKF. AIAA international space Planes and hypersonic systems and technologies conference. https://doi.org/10.2514/6.2011-2385

Esfahani PM, Lygeros J (2016) A tractable fault detection and isolation approach for nonlinear systems with probabilistic performance. IEEE Trans Autom Control 61(3):633–647. https://doi.org/10.1109/tac.2015.2438415

Fang J, Sun H, Cao J, Zhang X, Tao Y (2011) A novel calibration method of magnetic compass based on ellipsoid fitting. IEEE Trans Instrum Meas 60(6):2053–2061. https://doi.org/10.1109/tim.2011.2115330

Feng Y B, Li X S, Zhang XJ (2015) Fault detection method for integrated navigation system of gyroscope and compass. Journal of instrument and meter 36:2381–2388.

Gao S, Zhong Y, Li W (2011) Robust adaptive filtering method for SINS/SAR integrated navigation system. Aerosp Sci Technol 15(6):425–430. https://doi.org/10.1016/j.ast.2010.08.007

Gao W, Zhang Y, Wang JG (2014) A strapdown interial navigation system/Beidou/Doppler velocity log integrated navigation algorithm based on a cubature Kalman filter. Sensors 14(1):1511–1527. https://doi.org/10.3390/s140101511

Hajiyev C (2012) Fault tolerant integrated radar/inertial altimeter based on nonlinear robust adaptive Kalman filter. Aerosp Sci Technol 17(1):40–49. https://doi.org/10.1016/j.ast.2011.03.005

Julier SJ, Uhlmann JK, Durrant-Whyte HF (2002) A new approach for filtering nonlinear systems. Proc Am Control Conf 3:1628–1632. https://doi.org/10.1109/acc.1995.529783

Le HX, Matunaga S (2014) A residual based adaptive unscented kalman filter for fault recovery in attitude determination system of microsatellites. Acta Astronautica 105(1):30–39. https://doi.org/10.1016/j.actaastro.2014.08.020

Li S, Li S, Pei R (2011) Multiple sets of INS fault detection based on information fusion. Int Conf Electron Meas Instrum 4:81–85. https://doi.org/10.1109/icemi.2011.6037952

Liang Y, Jia Y (2015) A nonlinear quaternion-based fault-tolerant SINS/GNSS integrated navigation method for autonomous UAVs. Aerosp Sci Technol 40:191–199. https://doi.org/10.1016/j.ast.2014.11.009

Mohajerin Esfahani P, Lygeros JA, Tractable (2015) Fault Detection and Isolation Approach for Nonlinear Systems with Probabilistic Performance. IEEE Transactions on Automatic Control 1–1. https://doi.org/10.1109/TAC.2015.2438415

Nørgaard M, Poulsen NK, Ravn O (2000) New developments in state estimation for nonlinear systems. Automatica 36:1627–1638. https://doi.org/10.1016/s0005-1098(00)00089-3

Poulsen NK, Ravn O (2000) New developments in state estimation for nonlinear systems. Pergamon Press, Inc. https://doi.org/10.1016/s0005-1098(00)00089-3

Ritz T, Wiltschko R, Hore PJ, Rodgers CT, Stapput K, Thalau P, Wiltschko W (2009) Magnetic compass of birds is based on a molecule with optimal directional sensitivity. Biophys J 96(8):3451–3457. https://doi.org/10.1016/j.bpj.2008.11.072

Sun F, Song H, Gao W (2005) Study of SINS/GPS/DVL integrated navigation system's fault tolerance. Mechatronics and automation. 2005 IEEE international conference, IEEE, 737–767. https://doi.org/10.1109/icma.2005.1626585

Wang XH (2009) Research on threshold selection principle based on sensor fault detection. Mech Eng Autom 2:105–106. https://doi.org/10.3969/j.issn.1672-6413.2009.02.041

Zhao B, Skjetne R, Blanke M, Dukan F (2014) Particle filter for fault diagnosis and robust navigation of underwater robot. IEEE Trans Control Syst Technol 22(6):2399–2407. https://doi.org/10.1109/tcst.2014.2300815

Zhen G, Feng S (2005) Research on integrated navigation method for auv. J Mar Sci Appl 4(2):34–38. https://doi.org/10.1007/s11804-005-0030-3

Zheng Q, Bian XQ (2006) Simulation platform of navigation system for autonomous underwater vehicle. J Mar Sci Appl 5(4):33–37. https://doi.org/10.1007/s11804-006-6024-y